

Modulating the Electrical Transport in the Two-Dimensional Electron Gas at LaAlO₃/SrTiO₃ Heterostructures by Interfacial Flexoelectricity

Fan Zhang,^{1,4} Peng Lv,² Yiteng Zhang,³ Shujin Huang,⁴ Chi-Man Wong,¹ Hei-Man Yau,¹ Xinxin Chen,¹ Zheng Wen,³ Xiaoning Jiang,⁴ Changgan Zeng,⁵ Jiawang Hong,^{2,†} and Ji-yan Dai^{1,*}


¹Department of Applied Physics, The Hong Kong Polytechnic University, Hung Hom, 999077 Kowloon, Hong Kong

²School of Aerospace Engineering, Beijing Institute of Technology, Beijing, 100081, People's Republic of China

³College of Physics, Qingdao University, Qingdao, 266071, China

⁴Department of Mechanical and Aerospace Engineering, North Carolina State University, Raleigh, North Carolina, 27606, USA

⁵International Center for Quantum Design of Functional Materials, Hefei National Laboratory for Physical Sciences at the Microscale, CAS Key Laboratory of Strongly Coupled Quantum Matter Physics, and Department of Physics, University of Science and Technology of China, Hefei, 230026, China

 (Received 29 December 2018; revised manuscript received 12 April 2019; published 26 June 2019; corrected 19 March 2020)

Thin film flexoelectricity is attracting more attention because of its enhanced effect and potential application in electronic devices. Here we find that a mechanical bending induced flexoelectricity significantly modulates the electrical transport properties of the interfacial two-dimensional electron gas (2DEG) at the LaAlO₃/SrTiO₃ (LAO/STO) heterostructure. Under variant bending states, both the carrier density and mobility of the 2DEG are changed according to the flexoelectric polarization direction, showing an electric field effect modulation. By measuring the flexoelectric response of LAO, it is found that the effective flexoelectricity in the LAO thin film is enhanced by 3 orders compared to its bulk. These results broaden the horizon of study on the flexoelectricity effect in the hetero-oxide interface and more research on the oxide interfacial flexoelectricity may be stimulated.

DOI: [10.1103/PhysRevLett.122.257601](https://doi.org/10.1103/PhysRevLett.122.257601)

Complex oxide interfaces are known to possess many novel physical properties because of their extraordinary electron systems [1,2] such as the two-dimensional electron gas (2DEG) in the LaAlO₃/SrTiO₃ (LAO/STO) heterostructure that was discovered in 2004 [3]. When a LAO thin film of >3 unit cell (u.c.) thick is epitaxially grown on TiO₂-terminated (001) STO, it results in a metallic interface, where high-mobility electrons are trapped [4]. The LAO/STO heterostructure is one of the most remarkable structures that has attracted a great deal of research interest because it possesses plenty of interesting physical phenomena and application potentials such as superconductivity [5], magnetism [6], and spin-orbital coupling effect [7], etc., at the interface. The formation mechanism of this 2DEG has been discussed in many works [8–11], among which the polar catastrophe is the most commonly discussed theory to explain the charge reconstruction across the heterostructure. The polar catastrophe model states that, in the LAO/STO heterostructure, 1/2 of the electrons on the LAO layer surface transfer to and are trapped at the interface to compensate the potential divergence accumulated by the alternately charged atomic layers in LAO [8].

To broaden the application potential of the LAO/STO 2DEG system, many efforts have been made to realize interfacial modulations through variant methods. In particular, spin field effect transistors [12], resistance switching [13], photon detection [14], gas sensing [15], and strain

modulation [16,17] have been demonstrated on this heterostructure. It is also expected that the strain gradient could realize subtle interfacial modulation on the LAO/STO heterostructure. As reported by Catalan *et al.*, the flexoelectricity can influence the free charge distribution in semiconductors, and the effective flexoelectric coefficient in BaTiO₃ is largely enhanced based on the barrier-layer mechanism [18]. In the LAO/STO heterostructure, the polar discontinuity induced interfacial conductivity renders the flexoelectricity a perfect platform to realize the idea that a polarity perturbation can induce modulations at the interface.

Bending-induced electricity, i.e., flexoelectricity, is a universal property possessed by all dielectric materials [19–21]. In contrast to piezoelectricity, which is the polarization induced by a homogenous strain, flexoelectricity is the polarization caused by a strain gradient, and can be characterized by the following equation [22]:

$$P_i = \mu_{ijkl} \frac{\partial \epsilon_{kl}}{\partial x_j}, \quad (1)$$

where the flexoelectric polarization P_i is proportional to the flexoelectric coefficient μ_{ijkl} and the strain gradient $\partial \epsilon_{kl} / \partial x_j$. This flexoelectric property is universal in all dielectric materials since it is not restricted by the crystal symmetry. The contribution to this flexoelectricity is the

breaking of the local lattice centrosymmetry, where the centers of net positive and negative charges are separated under a strain gradient. Another mechanism that can generate flexoelectricity is the asymmetric redistribution of the electron density, as it was found in single layer graphene [23,24]. It has also been found that flexoelectricity plays a central role in biological functions like the auditory systems [25] and bone repair and remodeling process [26]. Very recently, the strain gradient induced flexo-photovoltaic effect was discovered in centrosymmetric single crystals, which further demonstrated the modulation ability of flexoelectricity in oxide electronics [27].

In this work, we study the flexoelectric effect in LAO thin film on a STO substrate and its impact to the electrical transport properties of the interfacial 2DEG. By bending the LAO/STO sample in different directions, its interfacial resistance is manipulated to be an increase or decrease. A strain gradient induced flexoelectric field is found to greatly alter the electrical transport properties at the hetero-oxide interface in terms of carrier density and mobility change. It is also found that the effective flexoelectric coefficient of the LAO thin film is 3 orders higher than its bulk; this opens more possibilities in oxide thin film or heterostructure based device designing.

Experiments were designed to measure the interfacial resistance change when a strain gradient is introduced in the LAO/STO heterostructure, which was fabricated by growing 20 u.c.-thick LAO on the TiO₂-terminated (001) STO substrate by pulsed laser deposition (PLD). The interfacial electrical transport properties were measured from 2 to 300 K, which show identical 2DEG characteristics. Thin film deposition and electrical characterization details are provided in the Supplemental Material [28]. To ensure the symmetry of electrical transport property measurement configuration, a three-point mechanical bending fixture, as illustrated in Fig. 1, was used to induce strain gradient in the bar-shaped LAO/STO sample. Figure 1(a) shows the case of bending the sample upwards in an *n* shape, where the LAO film is on the tension side of the sample. The *u*-shape bending case is to place the sample upside down, where the LAO film is on the compression side of the sample. Figures 1(b) and 1(c) schematically illustrate our definitions of *n*-shape and *u*-shape bending, respectively. In the later discussions, this notation will be used for describing different bending directions. As shown by the opposite directions of the yellow arrows in the *n*-shape or *u*-shape bending state in Figs. 1(b) and 1(c), it is expected that the induced flexoelectric polarizations or electric fields will also have opposite signs and further induce different influence on the 2DEG at the LAO/STO interface.

As gradually increasing the deformation displacement w at the center of the sample, the change of interface resistance under different bending status with variant bending scales was recorded, and the results are

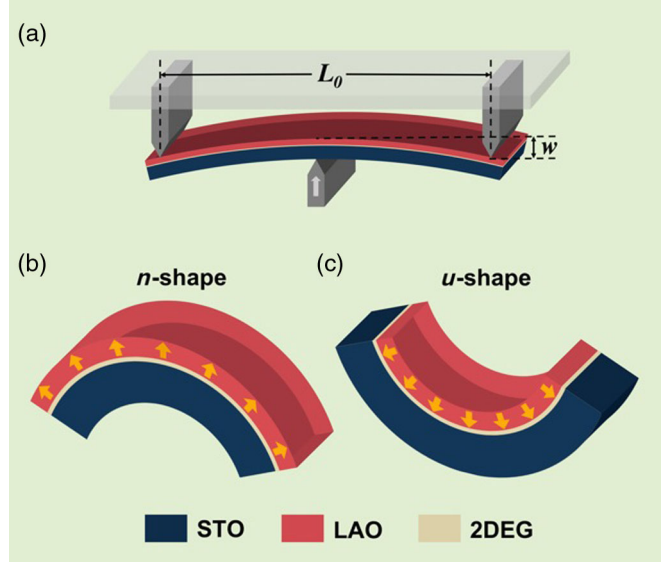


FIG. 1. Bending of the LAO/STO heterostructure. (a) The bending fixture setup for the three-point bending on LAO/STO samples. The sample illustrated is the *n*-shape bending status. Our definitions of the *n*-shape and *u*-shape bending are illustrated in (b) and (c), respectively. The yellow arrows represent the opposite flexoelectric polarizations in the LAO film under the two different bending status.

summarized in Fig. 2. The strain gradient is the value at the center of the sample and is calculated from the theory of elasticity [38,39]:

$$\frac{\partial \varepsilon_{11}}{\partial x_3} = 3w \left(\frac{L_0}{2} \right)^{-2}, \quad (2)$$

where L_0 and w , as noted in Fig. 1(a), represent the length of the sample's bending part and the deformation displacement of the sample's middle point, respectively. The strain gradient of *u*-shape bending is noted as negative, and the *n*-shape bending is noted as positive. In Fig. 2, R_0 is the resistance measured under a relaxed state, and the resistance change is calculated as the percentage of R_0 . It can be seen that the resistance increases as the *n*-shape bending scale increases, while it decreases as the *u*-shape bending scale increases. It is also apparent that the resistance changes proportionally to the strain gradient in both *n*-shape and *u*-shape bending cases. It is worth noting that when the bending force is relaxed, the resistance returns to its original value and can repeat the same level of resistance change under the same bending state. The error bars displayed in Fig. 2 are calculated from multiple measurements of more than two samples. As limited by the brittle nature of single crystals, the strain gradient cannot go further beyond the recorded values.

The flexoelectric modulation to the 2DEG is similar to ferroelectric control of conduction at the LAO/STO interface [40]. As depicted by yellow arrow in

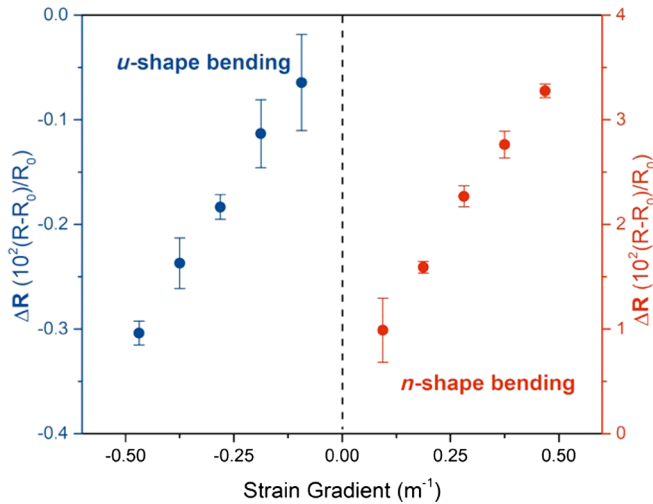


FIG. 2. The interface resistance change percentage under *u*-shape (negative strain gradient) and *n*-shape (positive strain gradient) bending. To illustrate the resistance change more obviously, the *y*-axis scale is adjusted according to the maximum resistance change values under the corresponding bending status.

Figs. 1(b) and 1(c), it is proposed that in such a hetero-oxide structure, when a strain gradient is introduced, a flexoelectric polarization is expected to be generated and alter the band diagram of the LAO film by coupling with its intrinsic polarization. As known, the formation of the interfacial 2DEG is induced by the diverged electrical potential accumulated by the alternately charged atomic layers (LaO^+ and AlO_2^-) in LaAlO_3 , which can be noted as its intrinsic polarization. The LAO is grown on TiO_2 -terminated STO, so the alternately charged atomic layers in LAO start with a positively charged LaO^+ layer, and the intrinsic polarization is pointing down (from LAO side to STO side). Under *u*-shape bending, the flexoelectric polarization in LAO is along the film's intrinsic polarization, and the potential divergence is enhanced by the flexoelectric field. This gives rise to electron accumulation at the interface and results in a decrease of interfacial resistance. By contrast, under *n*-shape bending, the LAO flexoelectric polarization is in an opposite direction of its intrinsic polarization, and electrons will be expelled from the interface to cause a resistance increase. A schematic illustration of the energy band diagram change is shown in Fig. S5 in the Supplemental Material [28]. The first-principles calculations were also conducted trying to understand the origin of the interfacial resistance change, and as shown in Fig. S7, the carrier density change at the interface is in agreement with interfacial resistance change. The carrier density change is attributed to the total polarization change which is the superposition of the LAO intrinsic polarization and the flexoelectric polarization from the *u*-shape and *n*-shape bending. More details about the DFT calculation are introduced in the Supplemental Material [28].

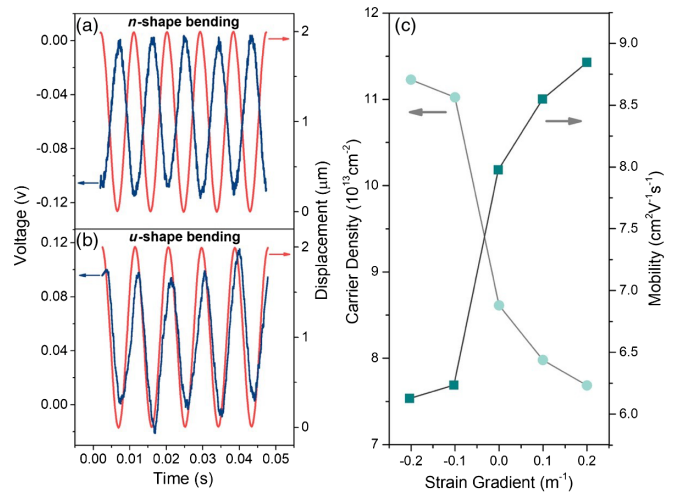


FIG. 3. The flexoelectric field effect across the LAO/STO heterostructure. The output voltage between the LAO/STO interface and the Au top electrode on LAO film surface under a periodic dynamic (a) *n*-shape bending and (b) *u*-shape bending. The blue curves are the voltage signal probed from the LAO/STO interface. The red curves are the bending displacement at the center of the sample. (c) The experimental interfacial electrical transport property change under different bending states: the circles are carrier densities and the squares are mobilities. The negative and positive strain gradients represent *u*-shape and *n*-shape bending, respectively. The corresponding sheet resistance change is shown in Fig. S4 of the Supplemental Material [28], where the strain gradient values are estimated from the sample's maximum bending limit.

To reveal the existence of such flexoelectric field across the LAO/STO heterostructure, the bending induced potential difference across the LAO layer was probed under a dynamic bending stimulation. (See Supplemental Material for measurement circuit [28].) As shown in Figs. 3(a) and 3(b), the output voltage follows the displacement in a periodical manner. In the *n*-shape bending case, the output voltage and force excitation is antiphase, suggesting that the interfacial electrons are expelled from the interface; this causes the interface resistance increase. In the *u*-shape bending case, the output voltage signal and force excitation is in phase, suggesting that the interface attracts more electrons; this causes the interface resistance decrease.

Flexoelectric polarization generates electric field, so the bending induced modulation to the 2DEG can be further explained in the scenario of electric field effect (EFE). The EFE modulations to the carrier density and mobility of the 2DEG at LAO/STO interface have been demonstrated through either front gating, back gating, or dual gating [4,41–46]. Under the *u*-shape (or *n*-shape) bending state, the flexoelectric polarization in the LAO layer is pointing towards (or away from) the interface and results in a positive (or negative) bound charge sheet at the bottom of the LAO. It is known that the 2DEG layer is located slightly below interface and has a thickness of a few nanometers

electrode. By growing LAO or STO film on (001)Nb:STO, we can directly measure the flexoelectric response of the LAO or STO film, and the results are also shown in Figs. 4(d) and 4(e). One can see that effective flexoelectric coefficient of the STO film on Nb:STO, i.e., $\mu_{12}^{\text{eff}}_{\text{STO-film}}$, is still in the same order of magnitude compared to its bulk. However, significantly enhanced flexoelectricity, i.e., $\mu_{12}^{\text{eff}}_{\text{LAO-film}}$, can be found in the LAO/Nb:STO sample which possess the same scenario of interfacial strain and strain gradient as the LAO/STO system. These results further suggest that the enhancement of thin film flexoelectricity in the LAO/STO heterostructure could be a consequence of the interfacial strain. In fact, it has been demonstrated that the electrical modulation capability in those nanoscale materials or thin films is usually much more obvious [59–63]. Nevertheless, the mechanism of the enhanced flexoelectricity in the LAO film deserves further investigations.

Before conclusion, it is worth mentioning that the in-plane strain the LAO layer and the LAO/STO interface experienced during bending might also influence the 2DEG. Our previous work revealed the resistance change at the LAO/STO interface induced by homogeneous strain, but only less than 0.1% by a strain of about 0.2% [17,64]. The surface compressive or tensile strain under the maximum bending scales shown in Fig. 2 can be estimated by multiplying the strain gradient ($\geq 0.5 \text{ m}^{-1}$) by half of the sample thickness ($0.5 \text{ mm} \times 0.5$); this results in a surface strain less than 0.125%, which is much smaller than the previous work. Compared to the 3% interfacial resistance change induced by bending, the in-plane strain effect can be neglected. Therefore, it is believed that bending induced strain gradient and flexoelectricity dominates the influence to the electrical transport property modulation. Other report also suggests the existence of flexoelectricity in the LAO/STO system, where interfacial conductivity modulation is realized by the tip pressing force of the scanning probe microscope (SPM) [63]. However, as reported, the oxygen vacancy migration induced by the SPM tip pressing is nonrecoverable until an electrical bias is applied. By contrast, in our work, recoverable modulation can be achieved, allowing us to quantitatively and macroscopically demonstrate the flexoelectric effect in the LAO/STO heterostructure and its modulation to the interfacial electrical transport properties. This makes the flexoelectric effect in this 2DEG promising for device applications such as mechanical sensing, energy harvesting, and flexoelectricity enhanced photovoltaics.

In summary, by inducing a strain gradient to the LAO/STO heterostructure, large electrical transport modulation to the interfacial 2DEG has been realized. The interfacial resistance increases during *n*-shape bending and decreases during *u*-shape bending, and the enhanced interfacial flexoelectricity is believed to play a crucial role in a scenario of electric field effect modulation.

Coupled with intrinsic polarization of the LAO thin film, flexoelectric polarization shows its ability to stimulate an electron density and mobility change at the interfacial 2DEG. This result illustrates how the flexoelectricity can influence the complex oxide interface based electronic devices, and opens new possibilities for device design based on complex oxide thin films and heterostructures.

This work was supported by the Hong Kong RGC Research Scheme (Grant No. N-PolyU517/14) and The Hong Kong ITF Grant (No. ITS044/17). J. H. acknowledges support from the National Science Foundation of China (Grant No. 11572040), the Thousand Young Talents Program of China. Z. W. acknowledges support from the Special Funds of the Taishan Scholar Program of Shandong Province (tsqn201812045). C. Z. acknowledges support from the National Natural Science Foundation of China (Grant No. 11434009). Theoretical calculations were performed using resources of the National Supercomputer Centre in Guangzhou, which is supported by the Special Program for Applied Research on Super Computation of the NSFC-Guangdong Joint Fund (the second phase) under Grant No. U1501501.

F. Z. and P. L. contributed equally to this work.

*Corresponding author.

jijian.dai@polyu.edu.hk

hongjw@bit.edu.cn

- [1] H. Y. Hwang, Y. Iwasa, M. Kawasaki, B. Keimer, N. Nagaosa, and Y. Tokura, Emergent phenomena at oxide interfaces, *Nat. Mater.* **11**, 103 (2012).
- [2] J. Mannhart and D. G. Schlom, Oxide interfaces—an opportunity for electronics, *Science* **327**, 1607 (2010).
- [3] A. Ohtomo and H. Y. Hwang, A high-mobility electron gas at the $\text{LaAlO}_3/\text{SrTiO}_3$ heterointerface, *Nature (London)* **427**, 423 (2004).
- [4] S. Thiel, G. Hammerl, A. Schmehl, C. W. Schneider, and J. Mannhart, Tunable quasi-two-dimensional electron gases in oxide heterostructures, *Science* **313**, 1942 (2006).
- [5] N. Reyren *et al.*, Superconducting interfaces between insulating oxides, *Science* **317**, 1196 (2007).
- [6] A. Brinkman, M. Huijben, M. van Zalk, J. Huijben, U. Zeitler, J. C. Maan, W. G. van der Wiel, G. Rijnders, D. H. A. Blank, and H. Hilgenkamp, Magnetic effects at the interface between non-magnetic oxides, *Nat. Mater.* **6**, 493 (2007).
- [7] E. Lesne *et al.*, Highly efficient and tunable spin-to-charge conversion through Rashba coupling at oxide interfaces, *Nat. Mater.* **15**, 1261 (2016).
- [8] N. Nakagawa, H. Y. Hwang, and D. A. Muller, Why some interfaces cannot be sharp, *Nat. Mater.* **5**, 204 (2006).
- [9] G. Herranz *et al.*, High Mobility in $\text{LaAlO}_3/\text{SrTiO}_3$ Heterostructures: Origin, Dimensionality, and Perspectives, *Phys. Rev. Lett.* **98**, 216803 (2007).
- [10] Z. Q. Liu *et al.*, Origin of the Two-Dimensional Electron Gas at $\text{LaAlO}_3/\text{SrTiO}_3$ Interfaces: The Role of Oxygen

- Vacancies and Electronic Reconstruction, *Phys. Rev. X* **3**, 021010 (2013).
- [11] M. Sing *et al.*, Profiling the Interface Electron Gas of LaAlO₃/SrTiO₃ Heterostructures with Hard X-Ray Photoelectron Spectroscopy, *Phys. Rev. Lett.* **102**, 176805 (2009).
- [12] N. Reyren, M. Bibes, E. Lesne, J. M. George, C. Deranlot, S. Collin, A. Barthélemy, and H. Jaffrès, Gate-Controlled Spin Injection at LaAlO₃/SrTiO₃ Interfaces, *Phys. Rev. Lett.* **108**, 186802 (2012).
- [13] C. Cen, S. Thiel, G. Hammerl, C. W. Schneider, K. E. Andersen, C. S. Hellberg, J. Mannhart, and J. Levy, Nano-scale control of an interfacial metal–insulator transition at room temperature, *Nat. Mater.* **7**, 298 (2008).
- [14] N. Y. Chan, M. Zhao, N. Wang, K. Au, J. Wang, L. W. H. Chan, and J. Dai, Palladium nanoparticle enhanced giant photoresponse at LaAlO₃/SrTiO₃ two-dimensional electron gas heterostructures, *ACS Nano* **7**, 8673 (2013).
- [15] N. Y. Chan *et al.*, Highly sensitive gas sensor by the LaAlO₃/SrTiO₃ heterostructure with Pd nanoparticle surface modulation, *Adv. Mater.* **26**, 5962 (2014).
- [16] C. W. Bark *et al.*, Tailoring a two-dimensional electron gas at the LaAlO₃/SrTiO₃ (001) interface by epitaxial strain, *Proc. Natl. Acad. Sci. U.S.A.* **108**, 4720 (2011).
- [17] F. Zhang, Y.-W. Fang, N. Y. Chan, W. C. Lo, D. F. Li, C.-G. Duan, F. Ding, and J. Y. Dai, Dynamic modulation of the transport properties of the LaAlO₃/SrTiO₃ interface using uniaxial strain, *Phys. Rev. B* **93**, 214427 (2016).
- [18] J. Narvaez, F. Vasquez-Sancho, and G. Catalan, Enhanced flexoelectric-like response in oxide semiconductors, *Nature (London)* **538**, 219 (2016).
- [19] A. K. Tagantsev, Piezoelectricity and flexoelectricity in crystalline dielectrics, *Phys. Rev. B* **34**, 5883 (1986).
- [20] P. Zubko, G. Catalan, and A. K. Tagantsev, Flexoelectric effect in solids, *Annu. Rev. Mater. Res.* **43**, 387 (2013).
- [21] L. E. Cross, Flexoelectric effects: Charge separation in insulating solids subjected to elastic strain gradients, *J. Mater. Sci.* **41**, 53 (2006).
- [22] J. Hong and D. Vanderbilt, First-principles theory and calculation of flexoelectricity, *Phys. Rev. B* **88**, 174107 (2013).
- [23] S. V. Kalinin and V. Meunier, Electronic flexoelectricity in low-dimensional systems, *Phys. Rev. B* **77**, 033403 (2008).
- [24] G. da Cunha Rodrigues, P. Zelenovskiy, K. Romanyuk, S. Luchkin, Y. Kopelevich, and A. Kholkin, Strong piezoelectricity in single-layer graphene deposited on SiO₂ grating substrates, *Nat. Commun.* **6**, 7572 (2015).
- [25] K. D. Breneman, W. E. Brownell, and R. D. Rabbitt, Hair cell bundles: Flexoelectric motors of the inner ear, *PLoS One* **4**, e5201 (2009).
- [26] F. Vasquez-Sancho, A. Abdollahi, D. Damjanovic, and G. Catalan, Flexoelectricity in bones, *Adv. Mater.* **30**, 1705316 (2018).
- [27] M.-M. Yang, D. J. Kim, and M. Alexe, Flexo-photovoltaic effect, *Science* **360**, 904 (2018).
- [28] See Supplemental Material at <http://link.aps.org/supplemental/10.1103/PhysRevLett.122.257601> for (i) thin-film deposition and characterization, (ii) mechanical bending fixture, (iii) band diagram under flexoelectric bending, (iv) effective flexoelectric coefficient measurement, and (v) DFT calculation, which includes Refs. [3,6,9,17,29–37].
- [29] S. R. Kwon, W. Huang, L. Shu, F.-G. Yuan, J.-P. Maria, and X. Jiang, Flexoelectricity in barium strontium titanate thin film, *Appl. Phys. Lett.* **105**, 142904 (2014).
- [30] S. Huang, T. Kim, H. Dong, D. Cann, J. L. Jones, and X. Jiang, Flexoelectric characterization of BaTiO₃-0.08Bi(Zn_{1/2}Ti_{1/2})O₃, *Appl. Phys. Lett.* **110**, 222904 (2017).
- [31] G. Kresse and J. Furthmüller, Efficient iterative schemes for *ab initio* total-energy calculations using a plane-wave basis set, *Phys. Rev. B* **54**, 11169 (1996).
- [32] G. Kresse and J. Furthmüller, Efficiency of *ab-initio* total energy calculations for metals and semiconductors using a plane-wave basis set, *Comput. Mater. Sci.* **6**, 15 (1996).
- [33] J. P. Perdew, K. Burke, and M. Ernzerhof, Generalized Gradient Approximation Made Simple, *Phys. Rev. Lett.* **77**, 3865 (1996).
- [34] I. I. Piyanzina, Y. V. Lysogorskiy, I. I. Varlamova, A. G. Kiiamov, T. Kopp, V. Eyert, O. V. Nedopekin, and D. A. Tayurskii, Analysis of electronic and structural properties of surfaces and interfaces based on LaAlO₃ and SrTiO₃, *J. Low Temp. Phys.* **185**, 597 (2016).
- [35] H. J. Monkhorst and J. D. Pack, Special points for Brillouin-zone integrations, *Phys. Rev. B* **13**, 5188 (1976).
- [36] W. Siemons, G. Koster, H. Yamamoto, W. A. Harrison, G. Lucovsky, T. H. Geballe, D. H. A. Blank, and M. R. Beasley, Origin of Charge Density at LaAlO₃ and SrTiO₃ Hetero-interfaces: Possibility of Intrinsic Doping, *Phys. Rev. Lett.* **98**, 196802 (2007).
- [37] A. Kalabukhov, R. Gunnarsson, J. Börjesson, E. Olsson, T. Claeson, and D. Winkler, Effect of oxygen vacancies in the SrTiO₃ substrate on the electrical properties of the LaAlO₃/SrTiO₃ interface, *Phys. Rev. B* **75**, 121404(R) (2007).
- [38] P. Zubko, G. Catalan, P. R. L. Welche, A. Buckley, and J. F. Scott, Strain-Gradient-Induced Polarization in SrTiO₃ Single Crystals, *Phys. Rev. Lett.* **99**, 167601 (2007).
- [39] P. Zubko, G. Catalan, P. R. L. Welche, A. Buckley, and J. F. Scott, Erratum: Strain-Gradient-Induced Polarization in SrTiO₃ Single Crystals, *Phys. Rev. Lett.* **100**, 199906(E) (2008).
- [40] V. T. Tra *et al.*, Ferroelectric Control of the conduction at the LaAlO₃/SrTiO₃ heterointerface, *Adv. Mater.* **25**, 3357 (2013).
- [41] C. Woltmann, T. Harada, H. Boschker, V. Srot, P. A. V. Aken, H. Klauk, and J. Mannhart, Field-Effect Transistors with Submicrometer Gate Lengths Fabricated from LaAlO₃-SrTiO₃-Based Heterostructures, *Phys. Rev. Applied* **4**, 064003 (2015).
- [42] M. Hosoda, Y. Hikita, H. Y. Hwang, and C. Bell, Transistor operation and mobility enhancement in top-gated LaAlO₃/SrTiO₃ heterostructures, *Appl. Phys. Lett.* **103**, 103507 (2013).
- [43] Z. Chen, H. Yuan, Y. Xie, D. Lu, H. Inoue, Y. Hikita, C. Bell, and H. Y. Hwang, Dual-gate modulation of carrier density and disorder in an oxide two-dimensional electron system, *Nano Lett.* **16**, 6130 (2016).
- [44] Z. Chen *et al.*, Carrier density and disorder tuned superconductor-metal transition in a two-dimensional electron system, *Nat. Commun.* **9**, 4008 (2018).

- [45] A. D. Caviglia, S. Gariglio, N. Reyren, D. Jaccard, T. Schneider, M. Gabay, S. Thiel, G. Hammerl, J. Mannhart, and J.-M. Triscone, Electric field control of the $\text{LaAlO}_3/\text{SrTiO}_3$ interface ground state, *Nature (London)* **456**, 624 (2008).
- [46] C. Bell, S. Harashima, Y. Kozuka, M. Kim, B. G. Kim, Y. Hikita, and H. Y. Hwang, Dominant Mobility Modulation by the Electric Field Effect at the $\text{LaAlO}_3/\text{SrTiO}_3$ Interface, *Phys. Rev. Lett.* **103**, 226802 (2009).
- [47] M. Basletic, J.-L. Maurice, C. Carrétéro, G. Herranz, O. Copie, M. Bibes, É. Jacquet, K. Bouzehouane, S. Fusil, and A. Barthélémy, Mapping the spatial distribution of charge carriers in $\text{LaAlO}_3/\text{SrTiO}_3$ heterostructures, *Nat. Mater.* **7**, 621 (2008).
- [48] K. Janicka, J. P. Velev, and E. Y. Tsymbal, Quantum Nature of Two-Dimensional Electron Gas Confinement at $\text{LaAlO}_3/\text{SrTiO}_3$ Interfaces, *Phys. Rev. Lett.* **102**, 106803 (2009).
- [49] O. Copie *et al.*, Towards Two-Dimensional Metallic Behavior at $\text{LaAlO}_3/\text{SrTiO}_3$ Interfaces, *Phys. Rev. Lett.* **102**, 216804 (2009).
- [50] M. Sing *et al.*, Profiling the Interface Electron Gas of $\text{LaAlO}_3/\text{SrTiO}_3$ Heterostructures with Hard X-Ray Photoelectron Spectroscopy, *Phys. Rev. Lett.* **102**, 176805 (2009).
- [51] A. K. Tagantsev, Electric polarization in crystals and its response to thermal and elastic perturbations, *Phase Transit.* **35**, 119 (1991).
- [52] J. Krupka, R. G. Geyer, M. Kuhn, and J. H. Hinken, Dielectric properties of single crystals of Al_2O_3 , LaAlO_3 , NdGaO_3 , SrTiO_3 , and MgO at cryogenic temperatures, *IEEE Trans. Microwave Theory Tech.* **42**, 1886 (1994).
- [53] C. Merckling, M. El-Kazzi, G. Delhayé, V. Favre-Nicolin, Y. Robach, M. Gendry, G. Grenet, G. Saint-Girons, and G. Hollinger, Strain relaxation and critical thickness for epitaxial LaAlO_3 thin films grown on SrTiO_3 (001) substrates by molecular beam epitaxy, *J. Cryst. Growth* **306**, 47 (2007).
- [54] P. R. Willmott *et al.*, Structural Basis for the Conducting Interface between SrTiO_3 and LaAlO_3 , *Phys. Rev. Lett.* **99**, 155502 (2007).
- [55] J. L. Maurice, C. Carrétéro, M. J. Casanove, K. Bouzehouane, S. Guyard, É. Larquet, and J. P. Contour, Electronic conductivity and structural distortion at the interface between insulators SrTiO_3 and LaAlO_3 , *Phys. Status Solidi A* **203**, 2209 (2006).
- [56] J. H. Haeni *et al.*, Room-temperature ferroelectricity in strained SrTiO_3 , *Nature (London)* **430**, 758 (2004).
- [57] N. Bickel, G. Schmidt, K. Heinz, and K. Müller, Ferroelectric Relaxation of the SrTiO_3 (100) Surface, *Phys. Rev. Lett.* **62**, 2009 (1989).
- [58] G. Singh-Bhalla, C. Bell, J. Ravichandran, W. Siemons, Y. Hikita, S. Salahuddin, A. F. Hebard, H. Y. Hwang, and R. Ramesh, Built-in and induced polarization across $\text{LaAlO}_3/\text{SrTiO}_3$ heterojunctions, *Nat. Phys.* **7**, 80 (2011).
- [59] G. Catalan, A. Lubk, A. H. G. Vlooswijk, E. Snoeck, C. Magen, A. Janssens, G. Rispens, G. Rijnders, D. H. A. Blank, and B. Noheda, Flexoelectric rotation of polarization in ferroelectric thin films, *Nat. Mater.* **10**, 963 (2011).
- [60] H. Lu, C. W. Bark, D. Esque de los Ojos, J. Alcalá, C. B. Eom, G. Catalan, and A. Gruverman, Mechanical writing of ferroelectric polarization, *Science* **336**, 59 (2012).
- [61] D. Lee, A. Yoon, S. Y. Jang, J. G. Yoon, J. S. Chung, M. Kim, J. F. Scott, and T. W. Noh, Giant Flexoelectric Effect in Ferroelectric Epitaxial Thin Films, *Phys. Rev. Lett.* **107**, 057602 (2011).
- [62] S. M. Park, B. Wang, S. Das, S. C. Chae, J.-S. Chung, J.-G. Yoon, L.-Q. Chen, S. M. Yang, and T. W. Noh, Selective control of multiple ferroelectric switching pathways using a trailing flexoelectric field, *Nat. Nanotechnol.* **13**, 366 (2018).
- [63] P. Sharma *et al.*, Mechanical tuning of $\text{LaAlO}_3/\text{SrTiO}_3$ interface conductivity, *Nano Lett.* **15**, 3547 (2015).
- [64] A. E. Clark, J. P. Teter, and O. D. McMasters, Magnetostriction “jumps” in twinned $\text{Tb}_{0.3}\text{Dy}_{0.7}\text{Fe}_{1.9}$, *J. Appl. Phys.* **63**, 3910 (1988).

Correction: The originally published Fig. 3(c) contained an error and has been replaced.